Study of Normal and Malignant White Blood Cells by Time Domain Dielectric Spectroscopy

Irina Ermolina, Yulia Polevaya, Yuri Feldman

Department of Applied Physics
Hebrew University of Jerusalem
Jerusalem, Israel

Ben-Zion Ginzburg

Plant Biophysical Laboratory
Institute of Life Science
Hebrew University of Jerusalem
Jerusalem, Israel

and Michael Schlesinger

Hubert H. Humprey Center of Experimental Medicine
and Cancer Research
Hebrew University of Jerusalem
Hadassah Medical School, Jerusalem, Israel

ABSTRACT

The aim of this paper is to present a comprehensive theoretical and experimental study by means of time domain dielectric spectrometer (TDDS) of static and dynamic dielectric properties of normal and malignant blood cells. The successful use of the TDDS method as a tool of human cell study required a special protocol and algorithms for all stages of cell preparation, measurements and data treatment. The routine developed in this study was used in the experimental analysis of nine lines of malignant, transformed and normal lymphocytes. It was shown that dielectric permittivity, capacitance and conductivity values of the cell membrane are higher for normal lymphocytes in comparison with malignant ones.

1 INTRODUCTION

THE study of dielectric properties of blood cancer cells is particularly interesting from the point of view of scientific and clinical applications [1]. Information about the dielectric permittivity and conductivity of cancer cells in the wide range of frequencies of applied electric fields can help promote the understanding of the nature of cancer and be useful for practical applications (*e.g.* for early cancer diagnostics, monitoring of drug treatment, *etc.*).

The cell suspension spectra are known to show a so-called β dispersion [2], which is observed in the frequency range of 100 kHz to 10 MHz and can be interpreted as the interface polarization. This dispersion is usually described in the framework of different mixture formulas and shelled models of particles [2–7]. In the case of biological cells, the interface polarization is connected to the dielectric permittivity and conductivity of the cell structural parts.

The dielectric parameters of structural parts of biological cells can be determined by the measurement of dielectric spectra of cellular suspensions and subsequent calculation using a suitable dielectric model. The development of the dielectric cell model consists of two main parts. The first part is the description of the suspension spectrum by one of the numerous so-called mixture models [5, 7–10]. The correct selection of the appropriate mixture formula in the case of cell suspension is a very important stage for the successful calculation of the single cell spectrum.

The second step of the analysis is the modeling of the single cell spectrum. The models all contain a large number of dielectric and geometric parameters, which leads to uncertainty in their determination during the fitting procedure. Moreover, one could argue that some of these parameters are not independent and should be obtained by additional methods.

In this paper we present the analysis of the appropriate mixture formulas and consideration of the simulated complex dielectric permit-

tivity spectra in order to discuss the number and sensitivity of independent parameters in the aforementioned models. The applicability of the developed procedure was illustrated by the TDDS study of nine human lymphoid cell lines. Dielectric spectroscopy of these lines has provided information on the effect of immortalization of these lines, such as by infection with Epstein-Barr Virus (EBV) and the effect of malignant transformation on the electric properties of the cells as compared with normal lymphocytes.

2 DIELECTRIC MODELS OF CELL AND CELL SUSPENSION

2.1 MIXTURE MODELS

Cell suspensions composed of different phases (suspending medium and cells with few interfaces) can, from a dielectric point of view, be considered as a classical heterogeneous system. Several basic theoretical models have been developed in order to describe the dielectric behavior of such complex materials. Depending on the concentration, the shape of the dispersed phase and the conductivity of both the media and disperse phase, different mixture formulas can be applied in order to describe the electric property of the system [5, 8, 11–13].

The theoretical description of the heterogeneous materials is usually expressed in terms of classical electrodynamics and based on the application of the Laplace equation to calculate the electrical potential inside and outside a dispersed spherical particle [8, 11]. The first original derivation of a mixture formula for spherical particles was accomplished by Maxwell [14] and was later extended by Wagner [15]. This Maxwell-Wagner (MW) theory of interfacial polarization usually can be applied successfully only for dilute dispersions of spherical particles. The dielectric permittivity of such a mixture can be expressed by the well-known relationship

$$\varepsilon^*_{\text{mix}} = \varepsilon^*_1 \frac{(2\varepsilon^*_1 + \varepsilon^*_2) - 2p(\varepsilon^*_1 - \varepsilon^*_2)}{(2\varepsilon^*_1 + \varepsilon^*_2) + p(\varepsilon^*_1 - \varepsilon^*_2)} \tag{1}$$

where $\varepsilon^*_{\text{mix}}$, ε^*_1 and ε^*_2 are the dielectric permittivities of the mixture, continuous phase and inclusions, respectively, and p is the volume fraction of inclusions. This formula can be simplified for the case of small volume fraction of inclusions to

$$\varepsilon^*_{\text{mix}} = \varepsilon^*_1 \left(1 + 3p \frac{\varepsilon^*_2 - \varepsilon^*_1}{2\varepsilon^*_1 + \varepsilon^*_2}\right) \tag{2}$$

Fricke [16] and then Sillars [17] have generalized the MW theory for the case of ellipsoidal particles. Bruggemann [18] and Hanai [19] in their series of papers extended the theory also for the case of concentrated disperse systems. For a system containing homogeneously distributed spherical particles Hanai found that the complex permittivity of the system is given by

$$p = 1 - \frac{\varepsilon^*_2 - \varepsilon^*_{\text{mix}}}{\varepsilon^*_2 - \varepsilon^*_1} \left(\frac{\varepsilon^*_1}{\varepsilon^*_{\text{mix}}}\right)^{\frac{1}{3}} \tag{3}$$

Another expression for concentrated disperse systems was proposed by Böttcher [20, 21]. In this approach for a uniform external field, the electric field within each component of the mixture is taken as equal to the field in a sphere with the dielectric properties of the component in a medium with the apparent dielectric permittivity of the heterogeneous mixture.

$$p \frac{\varepsilon^*_2 - \varepsilon^*_1}{\varepsilon^*_2 + 2\varepsilon^*_{\text{mix}}} = \frac{\varepsilon^*_{\text{mix}} - \varepsilon^*_1}{3\varepsilon^*_{\text{mix}}} \tag{4}$$

Recently in some papers devoted to dielectric spectroscopic study of blood cells, the mixture equation of Looyenga [22] was used [7]. To obtain this expression, Looyenga assumed that the dielectric permittivity of the heterogeneous system is equal to an apparent dielectric permittivity of a mixture composed of spheres that are heterogeneous themselves but have slightly different compositions from the main mixture. This approach resulted in a differential equation with the following solution [22]

$$\varepsilon^*_{\text{mix}} = \left[\left(\varepsilon_1^{*\frac{1}{3}} - \varepsilon_2^{*\frac{1}{3}}\right)(1-p) + \varepsilon_2^{*\frac{1}{3}}\right]^3 \tag{5}$$

This equation is independent of particle shape or specific interactions between the particles [21]. Moreover, there is no limitation whatsoever in the value of the inclusions volume fraction.

Another model of a mixture system was presented by Kraszewski *et al.* [10] recently, who considered the wave propagation in a heterogeneous medium. The approach was based on the assumption that a biphase suspension can be considered as a sum of infinite number of layers, each of thickness $\delta l \ll \lambda$, where λ is the free-space wavelength. The expression can be written as follows

$$\varepsilon_{\text{mix}}^{*\frac{1}{2}} = (1-p)\varepsilon_1^{*\frac{1}{2}} + p\varepsilon_2^{*\frac{1}{2}} \tag{6}$$

All models described above are applicable for different mixture conditions depending on the condensed state, volume fraction, conductivity of the inclusions and the media, *etc.*

2.2 COMPARISON OF THE MIXTURE MODELS

In order to choose the most appropriate mixture model for the description of cell suspensions, a comparison was performed of the mixture models presented above (Equations (1) to (6)). All models were simulated with the fixed parameters of the suspending medium. Note, that the complex dielectric permittivity of the medium is presented as follows

$$\varepsilon^*_1(\omega) = \varepsilon_1 - \mathrm{i}\frac{\sigma_1}{\omega\varepsilon_o} \tag{7}$$

In order to simulate the most appropriate spectrum $\varepsilon^*_2(\omega)$ of blood cells considered here as an embedded material, the double-shell model of lymphocyte was used (see $\varepsilon^*_c(\omega)$ Section 2.3).

Figure 1 shows the dielectric permittivity ε_s of suspensions as a function of volume fraction of inclusions (suspended particles) at the low frequency limit. For small volume fractions (p<0.15) most of the models (Equations (1) to (4)) give a similar result. This outcome can be explained easily, because all of these relations are based on the application of the Laplace equation to the calculation of the electrical potential inside and outside the dispersed spherical particle (MW-like models). The main assumption in all these approaches is that the characteristic sizes of the single-phase regions are much larger than the Debye screening length [23]. Provided that the dielectric permittivity and electric conductivity of the individual phases are known, the interfacial models enable us to calculate the frequency-dependent permittivity of the system. An essential feature of the interfacial polarization effect in complex

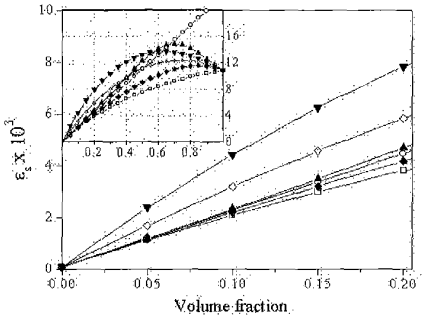

Figure 1. Static dielectric permittivity of suspensions as functions of volume fraction of inclusions (cells) calculated using different mixture formulas: (□) Maxwell-Wagner; (○) Maxwell-Wagner (short formula); (▲) Böttcher; (▼) Looyenga; (◊) Kraszewski; (♦) Hanai. The parameters of the suspending medium used in simulation are ε_1=65, σ_1=0.16 S/m. The complex dielectric permittivity of the embedded blood cells were calculated using the double-shell model with the parameters presented in Table 1.

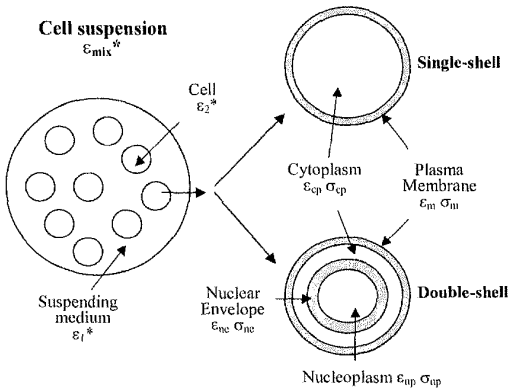

Figure 2. Schematic picture of the cell suspension, single and double-shell dielectric model of the cells. Every phase of the cell is described by the corresponding dielectric permittivity (ε) and conductivity (σ).

liquids with liquid-liquid interfaces is the appearance of an accumulated charge at the boundaries between differing dielectric media as a result of ionic migration processes [11, 12]. It is further assumed in the MW-like theory that the conductivities of each phase are uniform and constant. At the same time, the Looyenga equation [22] cannot be modified for application to conducting systems [21]. This is the reason that this model fails in the cell suspension description with comparatively high conductivity of the external medium. Cell suspensions also do not meet the requirements of the Kraszewski approach [10] because this model was derived for non-conductive layer, clay-sand like, materials and is not valid for a conductive spherical dispersed suspension. Therefore, taking into account the electrical and morphological properties of the dilute blood cell suspension, the MW model (See Equation (2)) can be used as the most appropriate for the single cell spectrum calculation.

2.3 SHELLED MODELS AND DOUBLE SHELL MODEL OF THE LYMPHOCYTES

It is well known that lymphocytes have a spherical shape, a thin cell membrane and spherical nucleus, which occupies ~ 60% of the cell volume and has a thin nuclear envelope [24]. Therefore, the dielectric properties of lymphocytes can be described by the double-shell model [4, 24, 25] (see Figure 2). In this model the cell is considered to be a conducting sphere covered with a thin shell, much less conductive than the sphere itself, in which a smaller sphere with a shell is incorporated. In addition, one assumes that every phase has no dielectric loss and that the complex dielectric permittivity can be written as

$$\varepsilon_i^*(\omega) = \varepsilon_i - \mathrm{i}\frac{\sigma_i}{\omega\varepsilon_o} \tag{8}$$

where ε_i is static permittivity and σ_i is the conductivity of every cell phase; i is the imaginary unit and ε_o the dielectric permittivity of free space. The subscript i can denote m for membrane, cp for cytoplasm, ne for nuclear envelope and np for nucleoplasm.

The effective complex dielectric permittivity ε_c^* of the whole cell is represented as a function of the phase parameters: complex permittivities of cell membrane ε_m^*, cytoplasm ε_{cp}^*, nuclear envelope ε_{ne}^*, and nucleoplasm ε_{np}^* [5, 24, 4].

$$\varepsilon_c^* = \varepsilon_m^* \frac{(1-\nu_1)+(1+2\nu_1)E_1}{(2+\nu_1)+(1-\nu_1)E_1} \tag{9}$$

where the geometrical parameter ν_1 is given by $\nu_1 = (1 - d/R)^3$, d is the thickness of plasma membrane, and R is the outer cell radius. The intermediate parameter E_1 is given by

$$\begin{aligned} E_1 &= \frac{\varepsilon_{cp}^*}{\varepsilon_m^*}\frac{2(1-\nu_2)+(1+2\nu_2)E_2}{(2+\nu_2)+(1-\nu_2)E_2} \\ \nu_2 &= \left(\frac{R_n}{R-d}\right)^3 \end{aligned} \tag{10}$$

where R_n, is the outer radius of nucleus. Finally, E_2 is given by

$$\begin{aligned} E_2 &= \frac{\varepsilon_{ne}^*}{\varepsilon_{cp}^*}\frac{2(1-\nu_3)+(1+2\nu_3)E_3}{(2+\nu_3)+(1-\nu_3)E_3} \\ \nu_3 &= \left(1-\frac{d_n}{R_n}\right)^3 \\ E_3 &= \frac{\varepsilon_{np}^*}{\varepsilon_{ne}^*} \end{aligned} \tag{11}$$

where d_n is the thickness of the nuclear envelope. In the case of prokaryotic cells (cells without nucleus) the single shell model is used. This model can be described by Equation (9), where $E_1 = \varepsilon_{cp}^*/\varepsilon_m^*$.

3 ANALYTICAL AND COMPUTER ANALYSIS OF APPLIED MODELS

3.1 NUMBER OF FITTING PARAMETERS

The dielectric properties of lymphocytes (eukariotic cells) usually are described by a double shell model which contains eleven parameters. It is important to estimate how many parameters are independent and which of them are preferable to fix in the treatment procedure. We

performed this analysis firstly for a single shell model with five parameters and then extrapolated the results for an analysis of a double shell model.

3.1.1 NUMBER OF FITTING PARAMETERS FOR THE SINGLE SHELL MODEL

The expression for the complex dielectric permittivity $\varepsilon_c^*(\omega)$ in the single shell model contains five parameters: dielectric permittivity and conductivity of the cell membrane ε_m and σ_m; dielectric permittivity and conductivity of the cell interior (cytoplasm) ε_{cp} and σ_{cp}, and a geometrical parameter $\nu = (1 - d/R)^3$ where d is the thickness of the cell membrane and R is the radius of the cell (see Equation (9)).

It is possible to show that the single shell model equation can be written as the sum of a single relaxation time process (Debye-type [1]) and a conductivity term. This equation depends only on four parameters (dielectric strength, relaxation time, dielectric permittivity at high frequency, and low frequency conductivity), which are functions of the dielectric and geometric properties of the single shell model. This connection between the Debye-type spectrum and the single shell model formulas allows one to conclude that only four independent parameters are required to describe the spectrum of a single cell. The fifth one can be expressed in terms of these four parameters. This expression can be derived by using the single shell model relation (Equation (9)) in the range of low and high frequencies. Let us rewrite Equation (9) as follows

$$\varepsilon_c^*(\omega) = \varepsilon_m^*(\omega)\left(\frac{1+2\nu}{1-\nu}\right)\left(\frac{1+A}{1+B}\right)$$
$$A = 2\frac{1-\nu}{(1+2\nu)E(\omega)} \qquad (12)$$
$$B = \frac{2+\nu}{(1-\nu)E(\omega)}$$

Our estimation, by using realistic parameters of cells, has shown that the frequency behavior of parameters A and B, in the range of $\sim 10^4$ to 10^{10} Hz for biological cells, demonstrate the following intervals of their variations: $10^{-8} < |A| < 10^{-4}$ and $10^{-2} < |B| < 10^2$.

Since parameter A is very small over a considerable frequency range it can be neglected and Equation (12) could be rewritten as follows

$$\varepsilon_c^*(\omega) = \varepsilon_m^*(\omega)\left(\frac{1+2\nu}{1-\nu}\right)\left(\frac{1}{1+B}\right) \qquad (13)$$

At the very low frequency branch the parameter B is very small and can be neglected. Hence, the low-frequency behavior of complex dielectric permittivity can be presented as

$$\varepsilon_{c(l)}^*(\omega) \simeq \varepsilon_m\left(\frac{1+2\nu}{1-\nu}\right) - \mathrm{i}\frac{\sigma_m}{\omega\varepsilon_o}\left(\frac{1+2\nu}{1-\nu}\right) \qquad (14)$$

At the high-frequency branch the parameter $B \gg 1$ and after simple transformations the complex dielectric permittivity of the cell spectrum below the frequency $\omega_{cp} = \sigma_{cp}/(\varepsilon_{cp}\varepsilon_o)$ is

$$\varepsilon_{c(h)}^*(\omega) \simeq \varepsilon_{cp} - \mathrm{i}\frac{\sigma_{cp}}{\omega\varepsilon_o} \qquad (15)$$

Figure 3 shows such asymptotic behavior at low and high frequencies for the single shell model spectrum calculated by Equation (9), where $E_1 = \varepsilon_{cp}^*/\varepsilon_m^*$.

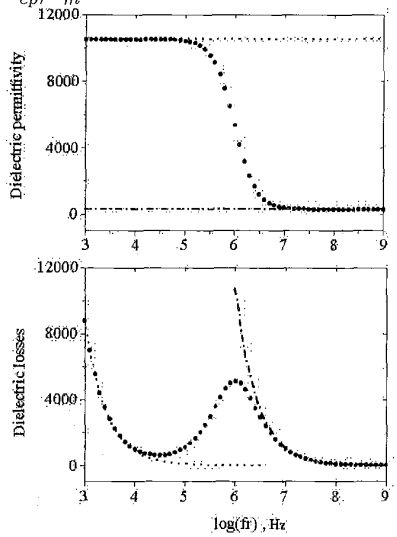

Figure 3. Single shell model spectrum (●) with its asymptotes of at low (dot line) and high (dash-dot line) frequencies.

Expressions (14) and (15) show that in the fitting procedure of the spectrum using the single shell model, the following set of four parameter combinations are obtained

$$\varepsilon_m\left(\frac{1+2\nu}{1-\nu}\right) \quad \sigma_m\left(\frac{1+2\nu}{1-\nu}\right) \quad \varepsilon_{cp} \quad \text{and} \quad \sigma_{cp} \qquad (16)$$

Here the first two terms indicate that one of three parameters ε_m, σ_m and ν must be obtained by an independent method and fixed during the fitting procedure, whereas the other two parameters can be fitted. Usually, the geometrical parameter ν is fixed, because it can be obtained by using the values of the cell radius R and the cell membrane thickness d, which are evaluated independently. The parameters ε_{cp} and σ_{cp} in the set (16) can be calculated directly from the fitting procedure.

It can be shown analytically that the expression for the model spectrum of a cell suspension, represented by the combination of the well-known Maxwell-Wagner mixture formula (Equation (2)) and the relation (9) for the single shell model, can be presented as the sum of two Debye-type processes and a conductivity term. This is in agreement with the ideas behind the work of Irimajiri [4] that every shelled particle interface gives a single Debye-type dispersion. In the case of a one-shell particle suspension there are two interfaces (cytoplasm – cell membrane and cell membrane – suspending medium interfaces). Hence, in the single shell particles two Debye-type dispersions should be observed. However, it was shown [6] that for biological cells these two dispersions degenerate to a single one. Indeed, our numerical model experiment has shown that the dielectric strength of the second, high frequency (HF) dispersion is ~ 2 to 3 orders of magnitude smaller than the dielectric strength of the low frequency one and can therefore be neglected.

3.1.2 NUMBER OF FITTING PARAMETERS FOR THE DOUBLE SHELL MODEL

The degeneration of high frequency dispersion in the spectrum of a single shell particle suspension, as described in the previous Section can be extrapolated to the more complicated system of cells with a shelled nucleus, described by the double shell model [24]. According to Equations (9) to (11), this model contains eleven parameters: conductivity and permittivity of every cell phase (membrane, cytoplasm, nuclear envelope and nucleoplasm) and three geometric parameters.

The same assumptions for omitting the HF dispersion of the one-shell (*i.e.* prokaryotic) cell can also be applied to the nucleus with an envelope (eukariotic cell). Thus, practically, every shell adds a single Debye-type dispersion to the spectrum. Therefore, the expression for the spectrum of a suspension of double shell particles can be described by the sum of two Debye-type dispersions and a conductivity term. The number of parameters has increased to six phenomenological parameters (two values of dielectric strength, two relaxation times, dielectric permittivity at high frequency and dc conductivity). Thus, it follows that six independent parameters are enough to describe the double shell cell suspension spectrum and therefore, only six parameters can be derived from applying the fitting procedure to the experimental spectrum. The other five parameters have to be obtained by some independent method and must be fixed during the fitting procedure.

3.2 COMPUTER SIMULATION OF DOUBLE SHELL MODEL

Analysis of dielectric and geometrical parameters for white blood cells was performed in order to simulate the spectrum of a double shell cell model. The intervals of cell phase parameter variations obtained from different experimental studies [7, 24–29] are presented in Table 1. The reference values used in the model spectrum are listed in the last column. Following Asami [24] that the volume of the nucleus is equal to 60% of the cell volume ($R_n = 0.6^{1/3}R$) and using the thicknesses and radii of structural cell parts (see Table 1), the geometrical parameters ν_1, ν_2, and ν_3 were calculated. The variation intervals of radii and thicknesses were estimated under the assumption that the experimental error does not exceed 50%.

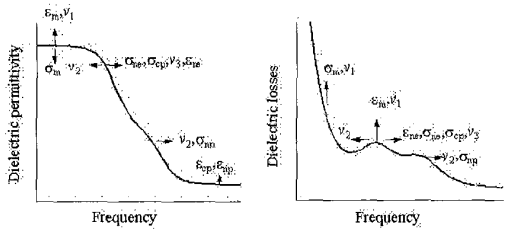

Figure 4. The influence of double shell model parameters on the cell spectrum. The arrows show the direction of spectrum changes. Symbols ε: dielectric permittivity, σ: dc conductivity. Subscripts m: cell (plasma) membrane, cp: cytoplasm, ne: nuclear envelope, np: nucleoplasm. ν_1, ν_2, ν_3 are the geometrical parameters of model.

The parameters were changed individually in order to evaluate their influence on the simulated spectrum. The variations of the values were implemented either in the framework of the limits in Table 1 or by noticeable spectrum alteration. The schematic presentation of the position and extent of the influence of each parameter on the double shell model spectrum is summarized in Figure 4. The detailed description of the model parameters and their influence on cell spectrum was discussed elsewhere [30], where it was shown that the plasma membrane permittivity demonstrate the maximum effect on the spectrum. The envelope permittivity has a moderate influence, and the permittivities of the cytoplasm and nucleoplasm almost do not affect the shape of the spectrum. Concerning the conductivities of the cell phases (plasma membrane, cytoplasm, nuclear envelope and nucleoplasm), all have a strong influence on different parts of the cell spectrum. The effect of the geometrical parameters ν_1, ν_2 and ν_3 was tested over a small range, which results from the range of variation for R, R_n, d and d_n for biological cells. Even small variations of these parameters produce a noticeable change in the spectral shape [30].

Table 1. The variation interval of cell phase parameters in double-shell model ε dielectric permittivity, σ dc conductivity (S/m), subscripts: m cell (plasma) membrane, cp cytoplasm, ne nuclear envelope, np nucleoplasm.

Parameters	Experimental limits		Reference
	lower	upper	parameter
ε_m	1.4	16.8	5.8
σ_m	8×10^{-8}	5.6×10^{-5}	8.7×10^{-6}
ε_{cp}	60	77	60
σ_{cp}	0.033	1.1	0.48
ε_{ne}	6.8	100	41
σ_{ne}	8.3×10^{-5}	7×10^{-3}	3×10^{-3}
ε_{np}	32	300	120
σ_{np}	0.25	2.2	0.95
R	3.5×10^{-6}	10.5×10^{-6}	7×10^{-6}
R_n	2.95×10^{-6}	8.85×10^{-6}	5.9×10^{-6}
d	3.5×10^{-9}	10.5×10^{-9}	7×10^{-9}
d_n	2×10^{-8}	6×10^{-8}	4×10^{-8}
ν_1	0.98805	0.999	0.99703
ν_2	0.4	0.8	0.60398
ν_3	0.95183	0.99043	0.99

Figure 4 shows that ε_m, σ_m and ν_1 affect the low frequency part of the spectrum; σ_{ne}, σ_{cp} and ν_3 affect the low frequency dispersion; ε_{ne}, and σ_{np} affect the high frequency dispersion; ν_2 has an influence on both dispersions; and ε_{cp}, ε_{np} affect the high frequency part of the spectrum. Hence, the dielectric parameters of the exterior cell phases influence the low frequency part of the spectrum, whereas the dielectric parameters of the interior cell phases affect the high frequency region.

The analysis presented above allows formulating the criteria for the optimal choice of fixed parameters in the fitting procedure of the cell spectrum. When several parameters influence the spectrum within the same frequency interval, some of them must be fixed. From this point of view all geometrical parameters (ν_1, ν_2, ν_3) can be fixed, moreover they can be measured independently. Due to the high sensitivity of the spectrum to ν_1, ν_2 and ν_3, it is important to evaluate them accurately.

The minimal distortion of the simulated spectrum due to significant variations of the model parameters can be another useful criterion for the selection of fixed parameters. Two parameters, ε_{cp} and ε_{np}, satisfy to this requirement in the best way. The analysis of cell dielectric models presented above allowed us to develop a special protocol and

algorithms for all stages of cell preparation, measurements and data treatment.

4 MATERIALS AND METHODS

4.1 SAMPLE PREPARATION

The following nine cell populations were investigated: normal peripheral blood T cells, normal tonsillar B cells, peripheral blood B cells which were transformed by infection with Epstein-Barr Virus (EBV) (Magala line), malignant B cell lines (Farage, Raji, Bjab, Daudi) and malignant T cell lines (Peer and HDMAR). The growth of cell lines, the isolation of peripheral blood T cells and selection of tonsillar B lymphocytes was performed in the laboratory of M. Schlesinger (Hebrew University, Hadassa Medical School).

For dielectric measurements the cells of each population were resuspended in a solution, which consisted of 229 mM sucrose, 16 mM glucose, 1 μM $CaCl_2$, and 5 mM Na_2HPO_4 in double distilled water (DDW). This solution had a low value of dc conductivity, isotonic osmotic pressure (280 mosmol) and pH=7.4.

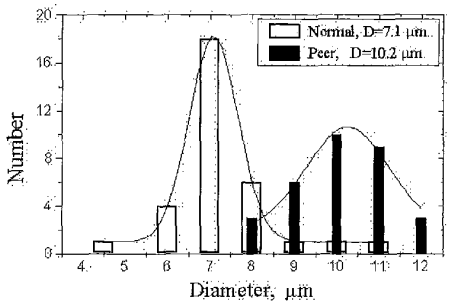

Figure 5. Typical size distributions for normal and malignant lymphocytes. The results of fitting by the Gauss distribution function are shown by the solid line. D is the mean diameter of cells.

The sizes of the cells were determined by an optical microscope. The typical size distribution is shown in Figure 5. The volume fractions were measured with a micro-centrifuge (Haematocrit) and corrected for the intercellular space, which was determined with Dextran Blue, and found to be 20.2±3.2% of the volume of the pellet [31, 32]. The main characteristics of the cell lines measured by independent methods are presented in Table 2. All measurements were performed at 25°C.

4.2 TIME DOMAIN DIELECTRIC SPECTROSCOPY

The dielectric properties of lymphocyte suspensions were determined with a commercial time domain dielectric spectrometer (TDDS), manufactured by Dipole TDS, Jerusalem. The general principles of time domain dielectric spectroscopy and a detailed description of the setup and procedure of our measurements were described elsewhere [33]. The spectrometer determines the dielectric properties of materials by measuring the response of a sample to an applied rapidly increasing pulse of electric field. In the framework of lumped capacitance approximation the complex dielectric permittivity is written as follows

Table 2. List of the cell populations studied. * Tonsillar B-cells, ** Peripheral blood T-cells. r radius, N number of experiments, and p is the volume fraction of the suspension.

Cells	r μm	N	p %
B-cells			
B-normal*	3.3	3	1.7→3.2
Magala	5.3	2	5.2→7
Farage	5.2	5	4.4→8.56
Raji	6.4	4	4.4→6.96
Bjab	6.3	3	2→6.4
Daudi	6.8	4	2.8→6.2
T-cells			
T-normal**	3.4	2	4
Peer	5.1	4	2.8→6.96
HDMAR	5.9	2	2.8→5.2

$$\varepsilon^*(\omega) = \frac{1}{i\omega C_0}\frac{L[I(t)]}{L[V(t)]} \tag{17}$$

where $I(t)$ is the current flow through the sample, $V(t)$ is the voltage applied to the sample, L is the Laplace transform operator, and C_0 is the capacitance of the empty coaxial sample cell which terminates the end of the coaxial line.

A small amount ($\sim 150\mu$L) of each cell suspension was used to fill the sample holder (the capacitance of the empty coaxial cell C_0=0.2 pF), and the time domain response of the sample was determined from the accumulation of 2560 individual signal records. Non-uniform sampling of the time window (5 μs) of each pulse enables the generation of spectra in the frequency range from 200 kHz to 3 GHz.

The most serious problem in TDDS measurements of conductive samples is the effect of electrode polarization. The accumulation of charge on electrode surfaces results in electrode polarization that leads to the formation of electrical double layers. The associated capacitance and complex impedance due to this polarization is so large that the correction for it is one of the major prerequisites in obtaining meaningful measurements on conductive samples, especially in aqueous biological and colloidal systems The detailed description of the electrode polarization correction is presented elsewhere [3, 28, 34].

5 RESULTS

The suspension spectra of the complex dielectric permittivity were measured by TDDS for 9 cell lines presented in Table 2. The single cell spectra were calculated using the Maxwell-Wagner mixture formula (2). The cell radius and volume fraction were measured independently. Typical examples of single cell spectra obtained for four of the cell lines studied are plotted in Figure 6. One can see that the spectra of various cell lines are different. The transition from a suspension spectrum to a spectrum of a single average cell leads to an increase of noise that is especially noticeable at high frequencies. This phenomenon results from the nonlinearity of Equation (2) and is reflected specially in the estimations of the nucleus envelope, cytoplasm and nucleoplasm parameters. Therefore these parameters were obtained with relatively low accuracy.

The spectrum of single cell was fitted to the double-shell model Equations (8) to (11). The experimental spectrum for Raji cell together with fitting curves, obtained by using both the single-shell and double-shell models presented as an example in Figure 7. Obviously, the single-

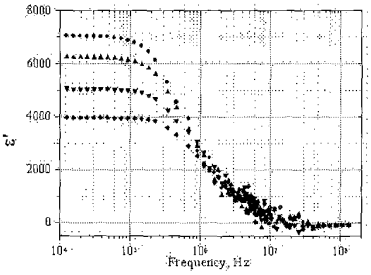

Figure 6. The real part of single cell dielectric permittivity spectrum for different cell populations calculated from experimental suspension spectra by Maxwell-Wagner mixture model; ●, Magala; ▲, Raji; ▼, Bjab; ♦, HDMAR.

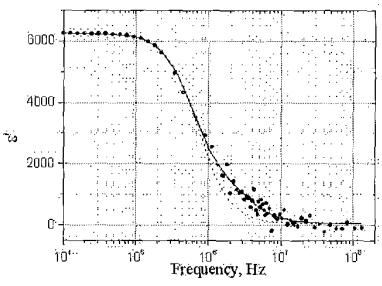

Figure 7. Fitting of Raji cell dielectric permittivity spectrum ●, to single-shell model (dashed line) and double-shell model (solid line).

shell model does not satisfy the description of experimental results, whereas the double-shell model corresponds properly to the spectrum.

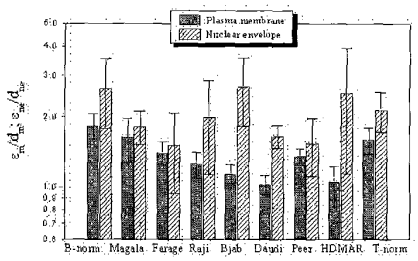

Figure 8. The dielectric permittivity divided by thickness for cell membrane ε_m/d_m, and nuclear envelope, ε_{ne}/d_{ne}, for studied cell lines.

The cell phase parameters obtained by fitting to the double shell model are presented in Table 3 and Figure 8. In the fitting procedure the following parameters were fixed: the cell radius R (see Table 2); the thickness of a cell membrane d=7 nm [24], the thickness of a nuclear envelope d_n=40 nm [24, 25], the ratio of a nucleus radius to a cell radius $R_n/R = (0.6)^{1/3}$; the dielectric permittivity of cytoplasm ε_{cp}=60 [24] and the dielectric permittivity of nucleoplasm ε_{np}=120. The last two parameters were chosen as a middle value from the literature [24, 25]. Note that according to our numerical evaluations and evidence [4, 25], the suspension spectrum is almost insensitive to the variation of ε_{cp}

Table 3. Dielectric parameters of cell structural parts for all cell populations studied. The fit was made by fixing the following parameters: ε_{cp}=60, ε_{np}=120, d=7 nm, d_n=40 nm, and $R_n = R \cdot (0.6)^{1/3}$.

Cells	ε_m ±12%	C_m μF/cm² ±12%	$10^{-6}\sigma_m$ S/m ±25%	ε_{ne} ±30%	C_{ne} μF/cm² ±30%	$10^{-3}\sigma_{ne}$ S/m ±30%	σ_{cp} S/m ±18%	σ_{np} S/m ±22%
B-cells								
B-normal	12.8	1.6	56	106	2.3	11.1	1.31	2.04
Magala	11.4	1.4	8.8	72.5	1.6	3.7	0.55	1.08
Farage	9.8	1.2	9.1	60.3	1.3	4.4	0.48	1.07
Raji	8.8	1.1	8.2	79.9	1.8	4.0	0.58	1.02
Bjab	8.0	1.0	11.0	108	2.4	2.1	0.88	1.39
Daudi	7.2	0.9	9.5	66.1	1.5	2.7	0.85	1.44
T-cells								
T-normal	11.1	1.4	27.4	85.6	1.9	8.8	0.65	1.26
Peer	9.5	1.2	12.9	61.6	1.4	2.1	0.81	1.42
HDMAR	7.4	0.9	14.5	101	2.2	3.0	0.88	1.58

and ε_{np} parameters over a wide interval of their values ($30 \div 300$). The values of the cell membrane and nuclear envelope capacitances were calculated by using the equation of a plate capacitor [35].

One can see (Table 3) that the membrane capacitance C_m, (or the similar parameter ε_m/d) has different values for the cell populations. These parameters for normal B cells exceed by 11% the values for the normal T cells. Even more dramatic is the difference between the value of the membrane capacitance of the normal cells and that for all the malignant cells. For B lymphocytes, the capacitance of the normal cells is higher than that of all the malignant cells. The same parameter for the EBV-transformed line (Magala) is intermediate between the values for normal and malignant cells. According to the statistical analysis by 't-test', the difference between transformed (Magala) and malignant lines is statistically significant whereas there is no statistically significant difference between the non-dividing (normal B) and transformed (Magala) populations. As for the T cell population, the membrane capacitance of the malignant cells (see Table 3 and Figure 8) was smaller than that of the normal T cells. However, this difference was borderline statistically significant.

The membrane conductivities σ_m, of normal cells of both the B and T populations were significantly higher than for that of malignant and transformed cells. In the B cell group, the membrane conductivity of normal cells was $\sim 6\times$ larger than that of the average value of the malignant cell lines and the transformed cell line. There was, however, no notable difference in the conductivity between the transformed and malignant cells in the B population. Concerning the conductivity of T cells, the difference between normal and malignant cells was not as remarkable as for B cells, but was statistically significant.

The dielectric permittivity of the nuclear envelope ε_{ne}, of normal B cells is $\sim 1.3\times$ larger than the average value of the cell lines of this group. The nuclear envelope conductivities σ_{ne}, in the B group are statistically higher in the normal cells than in all malignant B cell lines. The conductivity of the nuclear envelope of normal T cells is more than twice the average of this value in malignant cell lines.

The cytoplasm conductivity of normal B cells is larger by a factor of 1.8 than that of the average of the malignant cell lines. There is no difference in this parameter between the average of the malignant cell

lines and that of the transformed cell line. This parameter has almost the same value for both normal T and malignant T cells.

The nucleoplasm conductivity for normal B cells is larger by a factor of $\geqslant 1.6$ than that of the average value of the malignant cells, and this difference is statistically significant. In contrast, the nucleoplasm conductivity was slightly smaller in normal T cells than in malignant T cells. It is a very interesting fact that the conductivity of the nucleoplasm was about twice that for the cytoplasm for all cell populations.

6 DISCUSSION

The various dielectric parameters (see Table 3) of the cell populations presented in Table 2 were obtained for normal, EBV-transformed and malignant lymphocytes. Normal lymphocytes do not live for a prolonged time in culture and do not divide without addition of mitogenic stimuli. One of the methods used to immortalize lymphoid cells, so that they can live and divide under culture conditions, is to transform them with a virus such as the EBV-virus. The Magala B cell line was developed in this way. Transformed cells and malignant cells share the capacity to divide in culture. Malignant cells differ from normal and transformed cells by plenty of additional features. In our experiments both B and T cell populations could be characterized by two positive/negative properties, malignant or non-malignant nature of the cells (cancer/non-cancer), and the capacity to divide or lack of this capacity (dividing/non-dividing). Thus, the EBV-transformed Magala cells are non-cancerous but dividing, while Farage, Raji, Bjab, Daudi, Peer, and HDMAR lines are malignant and can divide in culture. In the framework of this classification of the cells and by using a t-test, the results can be summarized in the following way.

The specific cell membrane capacitance of cancer cell of B lines was lower than that of normal cells and of the EBV-transformed cell line (consisting of immortalized, dividing cell, that are not malignant). Thus it is clear that the decrease of the specific capacitance of the malignant B cells is strongly correlated with their cancerous feature rather than with their dividing mode.

There is a very noticeable decrease in the conductivity of cell membranes (by almost an order of magnitude) of the dividing cell lines (including the cancer lines and the transformed line). Thus, this property of the cell membrane seems to be correlated with dividing behavior of cells rather then with specific cancer features of the cells. May be the most important finding in our study is the very pronounced decrease of the electrical conductivity of the nuclear envelope of all the lines of dividing cells.

The average ionic composition of T and B human lymphocytes (consisting of Na^+, K^+, Cl^- and others) in the quiescent is consistent with the average conductivity of the cytoplasm and the nucleoplasm. Thus, as a first approximation our data on the conductivity of the inner cell solution are consistent with the assumption that the conductivity of the cytoplasm and the nucleoplasm is mainly due to the ionic species in aqueous media.

Yet the conductivity of the cytoplasm is invariably lower by a factor of 2, than that of the nucleoplasm. If the conductivity of either the cytoplasm and/or nucleoplasm, indeed, expresses mainly transport of small ions like Na^+, K^+, Cl^- in aqueous environment, then there must be a selective barrier between the two phases, which is very likely modified by the nuclear envelope. It is well known that the nuclear envelope has quite large pores. The nuclear pores are believed to regulate the bi-directional nucleocytoplasm transport of macromolecules, such as mRNA, transcription factors, proteins *etc.*, a process which is coupled to metabolic energy. It means that they indeed act as diffusion barriers. The open inner diameter of the pore was shown to be ~ 9 nm. The large diameter pore should lead to the conclusion that the nuclear pores are unable to regulate fluxes of ions (of dimensions of 0.3 to 0.4 nm) or maintain a gradient across the nuclear envelope. Recent studies claim to show ion channel activity at the nuclear envelope by using 'patch clamp' techniques [36, 37]. These findings put into focus the regulation of nuclear ions by the nuclear envelope. Several classes of K^+ selective ion-channels were recorded by patch-clamp techniques, with conductance of 100 to 550 pS in nuclei of different cells. Also a large, cation selective ion channels with maximum conductance of 800 pS in symmetrical 100 mM KCl was detected. This channel is a possible candidate for the open nuclear pore, because its conductance is consistent with the geometrical dimension of the open pore. But it is important to notice that this channel is open only for short times, and is mostly in the closing mode. This result is consistent with older data [36] on microelectrode studies with *in situ* nuclei, which claimed to measure a potential difference across the nuclear envelope and reported low electrical conductance of that membrane complex.

These findings on the nuclear envelope which act as diffusion barrier can explain the facts that the nucleoplasm and the cytoplasm can have a steady-state different conductivity and probably different compositions. As is shown in Table 3, the electrical conductivity of the nuclear envelope is larger by 2 orders of magnitude than of the cell membrane. We would then expect that the numbers of ionic channels and their nature, including their gating mechanism, would then be very different in these two types of cellular membranes.

ACKNOWLEDGMENT

We would like to thank Mrs. Rivka Hadar, Ms. Paloma Levy and Dr. Ruth Rabinowitz for their work on cell cultures and the separation of normal T and B cells. We are grateful to Prof. H. Ben-Bassat for the generous supply of various cell lines.

REFERENCES

[1] E. H. Grant, R. J. Sheppard and G. P. South, *Dielectric Behavior of Biological Molecules in Solution*, Claredon Press, Oxford, UK, 1978.

[2] H. P. Schwan, "Electrical properties of tissue and cell suspensions", Adv. Biol. Med. Phys., Vol. 5, pp. 147–209, 1957.

[3] R. Lisin, B.-Z. Ginzburg, M. Schlesinger and Yu. Feldman, "Time domain dielectric spectroscopy study of human cells. I. Erythrocytes and ghosts", Biochim. Biopys. Acta Vol. 1280, pp. 34–40, 1996.

[4] A. Irimajiri, T. Hanai and A. Inouye, "A dielectric theory of "Multi-Stratified Shell" model with its application to a lymphoma cell", J. Theor. Biol. Vol. 78, pp. 251–269, 1979.

[5] S. Takashima, *Electrical properties of biopolymers and membranes*, IOP Publishing Ltd, Philadelphia, USA, 1989.

[6] H. Pauly and H. P. Schwan, "Uber die Impedanz einer Suspension von kugelformigen Teilchen mit einer Schale", Z. Naturforsch Vol. 14 b, pp. 125–131, 1959.

[7] F. Bordi, C. Cametti, A. Rosi and A. Calcabrini, "Frequency domain electrical conductivity measurements of the passive electrical properties of human lymphocytes", Biochim. Biophys. Acta, Vol. 1153, pp. 77–88, 1993.

[8] T. Hanai, "Theory of the dielectric dispersion due to the interfacial polarization and its application to emulsions", Kolloid. Z., Vol. 171, pp. 23–31, 1960.

[9] J. Sjöblom, B. Jönsson, C. Nylander and I. Lundström, "Some dielectric properties of reversed micellar systems with different alkalicarboxylates and n-alcohols", J. Colloid. Interface Sci., Vol. 96, pp. 504–516, 1983.

[10] A. Kraszewski, S. Kulinski and M. Matuszewski, "Dielectric properties and a model of biphase water suspension at 9.4 GHz", J. Appl. Phys. Vol. 47, No. 4, pp. 1275–1277, 1976.

[11] S. S. Dukhin, V. N. Shilov, *Dielectric Phenomena, the Double Layer in Disperse Systems and Polyelectrolytes*, (translated by D. Lederman) Halsted Press, New York, 1974.

[12] R. Pethig, *Dielectric and Electronic Properties of Biological Materials*, John Wiley & Sons, Chichester, 1979.

[13] B. Nettelblad and G. A. Niklasson, "Dielectric relaxation in liquid-impregnated porous solids", J. Mater. Sci. Vol. 32, pp. 3783–3800, 1997.

[14] J. C. Maxwell, *A Treatise of Electricity & Magnetism*, articles 310–314 Dover, New York, 1954. (Originally Clarendon Press, 1891).

[15] K. W. Wagner, "Erklarung der dielectrischen Nachwirkungsvorgange auf Grund Maxwellscher Vorstellungen", Arch. Electrotech., Vol. 2, pp. 371–387, 1914.

[16] H. Fricke, "The Maxwell-Wagner dispersion in a suspension of ellipsoids", J. Phys. Chem., Vol. 57, pp. 934–937, 1953.

[17] R. W. Sillars, "The properties of a dielectric containing semiconducting particles of various shapes", J. Inst. Electr. Engrs., Vol. 80, pp. 379–394, 1937.

[18] D. A. G. Bruggemann, "Berechnung Verschiedenren Physicalischer Konstanten von Heterogenen Substanzen", Ann. Physik. Lpz., Vol. 24, pp. 636–679, 1935.

[19] T. Hanai, "Electrical Properties of Emulsions" in: *Emulsion Science*, (P. Sherman, ed.) Academic Press, New York, 1968.

[20] C. J. F. Böttcher, "The Dielectric Constant of crystalline powders", Rec. Trav. Chim., Vol. 64, pp. 47–51, 1945.

[21] C. J. F. Böttcher and P. Bordewijk, *Theory of Electric Polarization*, Elsevier, Amsterdam, The Netherland, 1978.

[22] H. Looyenga, "Dielectric Constants of heterogeneous mixture", Physica, Vol. 31, pp. 401–406, 1965.

[23] P. Debye and E. Hückel, "Zur Theorie der Electrolyte", Phys. Z., Vol. 24, pp. 185–206, 1923.

[24] K. Asami, Y. Takahashi and S. Takashima, "Dielectric properties of mouse lymphocytes and erythrocytes", Biochim. and Biophys. Acta, Vol. 1010, pp. 49–55, 1989.

[25] A. Irimajiri, Y. Doida, T. Hanai and A. Inouye, "Passive electrical properties of cultured murine lymphoblast (L5178 Y) with reference to its cytoplasmic membrane, nuclear envelope and intracellular phases", J. Mem. Biol. Vol. 38, pp. 209–232, 1978.

[26] C. Cametti, F. De Luca, M. A. Macri, B. Maraviglia, G. Zimatore, F. Bordi, R. Misasi, M. Sorice, L. Lenti and A. Pavan, "To what extent are the passive electrical parameters of lymphocyte membranes deduced from impedance spectroscopy altered by surface roughness and microvillosity", Colloids and Surfaces B: Biointerfaces, Vol. 3, pp. 309–316, 1995.

[27] A. Irimajiri, K. Asami, T. Ichinowatari and Y. Kinoshita, "Passive electrical properties of the membrane and cytoplasm of cultured rat basophil leukemia cells. I. Dielectric behavior of cell suspensions in 0. 01–500 MHz and its simulation with a single-shell model", Biochim. Biophys. Acta, Vol. 869, pp. 203–213, 1987.

[28] Yu. Polevaya, I. Ermolina, M. Schlesinger B.-Z., Ginzburg and Yu. Feldman, "Time domain dielectric spectroscopy of human cells. II. Normal and malignant white blood cells", Biochim. Biophys. Acta, Vol. 1419, pp. 257–271, 1999.

[29] H. Ziervogel, R. Glaser, D. Schadow and S. Heymann, "Electrorotation of lymphocytes - the influence of membrane events and nucleus", Bioscience Reports, Vol. 6, No. 11, pp. 973–982, 1986.

[30] I. Ermolina, Yu. Polevaya and Yu. Feldman, "Analysis of dielectric spectra of eukariotic cells by computer modeling", Eur. Biophys. J. and Lett., Vol. 29, pp. 141–145, 2000.

[31] M. Ginzburg and B.-Z. Ginzburg, "Distribution of non-electrolytes in Halobacterium cells", Biochim. Biophys. Acta, Vol. 584 pp. 398–406, 1979.

[32] A. Zmiri and B.-Z. Ginzburg, "Extracellular space and cellular sodium content in pellets of D. Parva (Dead Sea 75)", Plant Science letters, Vol. 30, pp. 211–218, 1983.

[33] Yu. Feldman, A. Andrianov, E. Polygalov, I. Ermolina, G. Romanychev, Yu. Zuev and B. Milgotin, "Time domain dielectric spectroscopy: An advanced measuring system", Rev. Sci. Instrum., Vol. 67, pp. 3208–3216, 1996.

[34] Yu. Feldman, R. Nigmatullin, E. Polygalov and J. Texter, "Fractal-polarization correction in time domain dielectric spectroscopy", Phys. Rev. E, Vol. 58, No 6, pp. 7561–7565, 1998.

[35] K. Asami, Y. Takahashi and S Takashima, "Frequency domain analysis of membrane capacitance of cultured cells (HeLa and myeloma) using the micropipette technique", Biophys. J., Vol. 58, pp. 143–148, 1990.

[36] A. J. M. Matzke and A. M. Matzke, "The electrical properties of the nuclear envelope and their possible role in the regulation of eukaryotic gene expression", Bioelectrochem. Bioenergetics, Vol. 25, pp. 357–370, 1991.

[37] J. O. Bustamente, "Nuclear electrophysiology", J. Mem. Biol., Vol. 138, pp. 105–112, 1994.

This manuscript is based on a paper given at the 10th International Symposium on Electrets, Delphi, Greece, 22–24 September 1999.

Manuscript was received on 14 February 2000, in final form 26 November 2000.